Submitted to Journal of Molecular Liquids

Biochar from byproduct to high value added material – a new adsorbent for toxic metal ions removal from aqueous solutions

Salvatore Cataldo[a], Vitaliano Chiodo[b], Francesco Crea[c], Susanna Maisano[b], Demetrio Milea[c] and Alberto Pettignano[a*]

[a] Dipartimento di Fisica e Chimica, Università di Palermo, Viale delle Scienze, I-90128 Palermo, Italy

[b] Institute CNR-ITAE, via Salita S. Lucia sopra Contesse 5, I-98126 – Messina, Italy

[c] Dipartimento di Scienze Chimiche, Biologiche, Farmaceutiche ed Ambientali, Università degli Studi di Messina, Viale Ferdinando Stagno d'Alcontres, 31, I-98166 Messina (Vill. S. Agata), Italy.

* Corresponding author: Tel: +39-091-23897959; Fax: +39-091-590015;

E-mail address: alberto.pettignano@unipa.it

ABSTRACT

An activated biochar coming from pyrolysis of dead *Posidonia oceanica* residues has been tested as adsorbent material for Cd^{2+}, Pb^{2+} and Cu^{2+} ions. The biomass, the activated and the non activated bio-chars were previously characterized by using several instrumental techniques. The pH of metal ion solution in kinetic and thermodynamic adsorption experiments was fixed at 5 whilst, the dependence on ionic medium, ionic strength and temperature have been evaluated carrying out batch experiments at different experimental conditions. Differential Pulse Anodic Stripping Voltammetry and Inductively Coupled Plasma Optical Emission Spectroscopy have been used to measure the metal ion concentration in the solutions. Several kinetic and isotherm equations were used to fit experimental data. The thermodynamic parameters ΔG, ΔH and ΔS of Pb^{2+} adsorption process were calculated by using Gibbs and van't Hoff equations.

A speciation study of the Pb^{2+} ion was also done in order to evaluate the influence of ionic medium, ionic strength and pH on the adsorption process. Information about adsorption mechanism was obtained from the analysis of thermodynamic parameters of adsorption and of the results of metal ions speciation and bio-char characterization.

Keywords: adsorption, toxic metals, biochar, speciation, *Posidonia oceanica*.

---

1. Introduction

The interest on biomass as alternative energy sources is greatly increased in the last decade. Biomass can be classified in i) lignocellulosic , ii) herbaceous and iii) aquatic flora and manure materials, and it can be converted into different forms of bio-fuels (solid, liquid and gaseous) through thermo-chemical and bio-chemical technologies. Recent studies propose the use of algal biomass in the production of bio-oil. In particular, pyrolysis of different algal species has been tested, including *Chlorella* [1], *Nannochloropsis* residue [2], *Sargassum* [3], *Spirulina* [4], *Synechococcus* [5], *Tetraselmis* [5,6] and the Mediterranean sea plant *Posidonia oceanica* [7,8]. Results concluded that pyrolysis of algal biomass is a promising process for renewable fuel production with a maximum oil yield of 54.97% at 773.15 K, and high heating values of 24-32 MJ kg^{-1}. Furthermore, effect of different catalysts on pyrolysis reactions have been also evaluated in order to improve the algae bio-oil quality; including Co/Al_2O_3, Ni/Al_2O_3, γ-Al_2O_3, CeO_2, Ni/CeO_2, ZSM-5, HZSM-5 [7–10]. However, when seaweed is used to make bio-oil, a large amount of biochar as byproduct is produced, with the consequent need to dispose it and the related disposal costs that make uneconomical the whole process. Moreover, the accumulation of this secondary product may cause solid waste pollution problems.

Independently of the origin, biochar is composed predominantly of amorphous carbon with a highly functionalized surface, which makes it reactive to various compounds, such as inorganic and organic species [11]. Thus, it is widely used for the removing and/or the immobilization of environmental contaminants such as toxic metal ions in aqueous and soil matrices [12–14].

52 The elemental composition of biochar and its properties vary according to the raw biomass material
53 from which it is produced and to the characteristics of the carbonization process [15]. Biochar
54 adsorption properties can be improved by physical or chemical activation treatments. In particular,
55 chemical activated biochar presents a greater adsorptive capacity towards organic and inorganic
56 compounds in relation to the material without chemical treatment, which can be directly related to
57 the increase of functional groups in the surface after the treatment [16,17].
58 In the last years, our research group undertook a systematic study on the adsorption ability towards
59 toxic metal ions of pristine and modified biomaterials, including a composite material of alginate
60 and active carbon [18–23].
61 In this context, the biochar coming from pyrolysis of a local waste biomass (the dead *Posidonia*
62 *oceanica* residues) (BCP) was chemically activated with sulfuric acid (see section 2.2) and
63 investigated for potential use as adsorbent of toxic metal ions. The raw material was previously
64 characterized [7,8] whilst, the BCP and the activated biochar (ABCP) have been characterized by
65 using different instrumental techniques. Considering the well known toxicity towards plants,
66 animals and humans, Pb^{2+}, Cd^{2+} or Cu^{2+} were chosen as metal ions to be removed in the batch
67 kinetic and thermodynamic adsorption experiments [24,25]. Depending on the origin, the
68 wastewater conditions (background, ionic strength, temperature), the subject of remediation
69 treatments, can vary considerably. For this reason, the adsorption isotherms were carried out in
70 different ionic media and at different ionic strengths and temperatures.
71 The ABCP recyclability has been tested carrying out several adsorption/desorption cycles on a fixed
72 amount of adsorbent material placed in a glass column.
73 The metal ions concentration in the solutions was measured by Differential Pulse Anodic Stripping
74 Voltammetry (DP-ASV) or Inductively Coupled Plasma Optical Emission Spectroscopy (ICP-OES)
75 techniques. The experimental data were fitted with several kinetic and isotherm equations. Gibbs
76 and van't Hoff equations were used to calculate the thermodynamic parameters ΔG, ΔH and ΔS of
77 Pb^{2+} adsorption.

Finally, the metal ions adsorption capacity of ABCP was compared with that of biochars produced from other biomasses and commercial activated carbons.

2. Experimental section

2.1 Materials

Sulphuric acid used in the BCP activation was prepared by diluting a concentrated Fluka solution. Cd^{2+}, Pb^{2+} and Cu^{2+} solutions were prepared by weighing the $Cd(NO_3)_2\,4H_2O$, the $Pb(NO_3)_2$ and the $Cu(NO_3)_2\,H_2O$ (Aldrich, analytical grade) salts, respectively. NaCl and $NaNO_3$ salts (Riedel-de Haën, puriss.) used to fix the ionic strength of the metal ion solutions at desired values was weighed after drying in oven at 383.15 K for 2 hours. Hydrochloric or nitric acids and sodium hydroxide solutions used to adjust the pH of the metal ion solutions and to calibrate the ISE-H^+ electrode were prepared by diluting concentrated Fluka solutions. Standard solutions of the toxic metal ions used for calibration curves were prepared by diluting 1000 mg L^{-1} standard solutions in 2 % HNO_3 (c ± 0,2% - trace select qualities, FLUKA). All the solutions were prepared using freshly, CO_2-free ultra pure water ($\rho \geq 18$ MΩ cm^{-1}) and grade A glassware.

2.2 Feedstock preparation, pyrolysis procedure, BCP activation and characterization

Posidonia oceanica leaf sheaths (Mediterranean sea-plant) were collected from the southwestern coast of Sicily region (Italy). The samples were washed with distilled water to remove sea salt, then dried in an oven (at 353.15 K for 24 h), shredded and conserved in a desiccator. Biomass samples were characterized by proximate and ultimate analyses, Higher Heating Values (HHV) and TGA/DTG analysis elsewhere reported [7].

BCP was prepared by carbonizing of about 100 g of dried *Posidonia oceanica* leaves through pyrolysis tests carried out in a stainless steel fixed bed reactor at three operative temperatures (673.15, 773.15 and 873.15 K) for 1 h; heating rate of 10 K min^{-1} and nitrogen flow (150 mL min^{-1}). Before each pyrolysis test, the reaction system was purged with N_2 for 60 min to eliminate inside

104 air. Condensable outlet gas stream (bio-oil) was condensed in three cold traps (195.15 K). The solid
105 residue (biochar) remained in the reactor was successively recovered and weighted. The amount of
106 gaseous products was calculated by subtracting the solid and liquid yields from the amount of initial
107 raw biomass. Conversion and product distribution yields of pyrolysis tests were calculated as in a
108 previous work [8]. All tests were performed in triplicate to evaluate the standard deviations.
109 The BCP was chemically activated following the procedure: 20 g of BCP were placed in an
110 Erlenmeyer flask with 500 mL of H_2SO_4 5 mol L^{-1} at 373.15 K and were stirred for 3 hours. After
111 activation treatment, the BCP was thoroughly washed with distilled water until the washing solution
112 has a pH ~ 5 and then dried in oven at 383.15 K.
113 The morphological features of the BCP and ABCP were examined by Scanning Electron
114 Microscopy (SEM) with a FEI XL30 microscope equipped with a field emission gun and EDX
115 probe, operating at an accelerating voltage of 20 kV.
116 The surface area, pore volume and average pore size of the BCP and of ABCP were analyzed by N_2
117 adsorption−desorption isotherm measurements at 77.35 K using the Micromeritics ASAP 2020
118 instrument. The Brunauer–Emmett–Teller (BET) total surface area was calculated from the
119 adsorption isotherm using the BET equation where monolayer coverage of nitrogen molecules is
120 assumed to be complete. While, the pore size distribution was estimated by using the Barret-Joyner-
121 Halenda (BJH) equation, during the desorption phase, and with the Horvath-Kawazoe method.
122 The pH of point zero charge of ABCP (pH_{pzc}) [26], was measured at I = 0.1 mol L^{-1}, in NaCl and
123 $NaNO_3$ media. For each ionic medium, 0.1 g of ABCP were placed in nine Erlenmeyer flasks
124 containing 50 mL of solution in the pH range 2 – 10. Purified N_2 gas was bubbled into each solution
125 for 10 min. After sealing with parafilm, the solution was magnetically stirred for 24 hours. The pH
126 of mixtures (final pH) was plotted against the pH of the initial solutions (initial pH) measuring the
127 pH_{pzc} as the intersection with blank curve.
128
129 ***2.3 Procedures for adsorption and desorption experiments***

The adsorption kinetic of Pb^{2+}, Cu^{2+} and Cd^{2+} ions onto ABCP was studied in $NaNO_3$ aqueous solution, at I = 0.1 mol L^{-1} and T = 298.15 K. The initial pH of the solution was adjusted at 5 and was monitored during the experiments. 0.04 g of ABCP were added to 25 mL of solution containing the metal ion ($C_{M^{2+}}$ = 30 mg L^{-1}) in a voltammetric cell under constant and regular stirring. The metal ion concentration in solution was measured at various adsorbent/solution contact times in the interval 0 - 24 h.

The isotherm experiments of Pb^{2+}, Cd^{2+} and Cu^{2+} adsorption onto ABCP were carried out in batch, at pH = 5. Approximately 200 mg of the adsorbent were placed in thermostatted cells containing each 25 mL of Pb^{2+}, Cd^{2+} or Cu^{2+} solution at different metal ion concentration ($10 \leq C_{M^{2+}}$ / mg $L^{-1} \leq 90$), in $NaNO_3$ at I = 0.1 mol L^{-1} and at T = 298.15 K. The dependence on ionic medium, ionic strength and temperature of Pb^{2+} adsorption onto ABCP was also studied carrying out the same batch experiments with solution containing NaCl medium, in the ionic strength range 0.1 – 1 mol L^{-1} and T = 298.15 K and in the temperature range 283.15 – 333.15 K in $NaNO_3$ 0.1 mol L^{-1}. The solutions were magnetically stirred for 24 hours and then were separated from the adsorbent before measuring the metal ion concentration and the pH.

The reuse and recycling of ABCP was studied packing 0.5 g of the adsorbent material into a glass column (diameter = 2 cm, length = 5 cm). Glass beads were placed on the top to prevent the movement of ABCP during the metal ion solution flow. 100 mL of Pb^{2+} solution ($C_{Pb^{2+}}$ = 60 mg L^{-1}, pH = 5, I(NaCl) = 0.1 mol L^{-1}) were flowed at reflux into the column with a flow rate of 12 mL min^{-1} for 24 hours (the reaching of adsorption equilibrium was verified) by using a peristaltic pump (Dulabo – PLP380). The ABCP was washed with distilled water before the Pb^{2+} desorption carried out with 100 mL of HNO_3 0.1 mol L^{-1} solution flowed in the column with the same flow rate and time (the reaching of desorption equilibrium was verified). Four adsorption/desorption cycles were done.

154 The metal ion concentration in the solutions coming from adsorption and desorption experiments
155 was measured by DP-ASV or by ICP – OES (Perkin Elmer Model Optima 2100, equipped with an
156 auto sampler model AS-90) techniques. The voltammetric apparatus was constituted by a Metrohm
157 663 VA stand combined with the Autolab potentiostat coupled with the IME663 interface. The
158 voltammetric apparatus was controlled by NOVA v. 1.10 software. The VA stand was equipped
159 with a three electrode system consisting of i) a Multi Mode Electrode Pro (Metrohm, code
160 6.1246.120) working in the Static Mercury Drop Electrode (SMDE) mode, ii) a glassy carbon
161 auxiliary electrode (code 6.1247.000), and iii) a double junction Ag/AgCl/KCl (3 mol L^{-1}) reference
162 electrode (code 6.0728.030). The DP-ASV measurements were performed after bubbling purified
163 N_2 gas into the solutions for 150 s. The experimental electrochemical conditions were chosen in
164 order to optimize signal/noise ratio, repeatability, accuracy and to avoid interferences and are
165 reported in Table 1S of supplementary material.
166 Calibration curves of Pb^{2+} and Cd^{2+} and Cu^{2+} ions were done at the same experimental conditions of
167 adsorption experiments. The pH of solutions was measured by a potentiometer equipped with a
168 combined ISE-H^+ glass electrode (Ross type 8102). The ISE-H^+ electrode was previously
169 calibrated, in the same experimental conditions of the adsorption experiments, titrating 25 mL of a
170 HNO_3 or HCl standard solution with NaOH. A potentiometric titration system (Metrohm, Model
171 888 Titrando) controlled by TIAMO software was used.
172
173 ***2.4 Models for kinetic and equilibrium adsorption studies and thermodynamic equations***
174 The adsorption kinetics of the three metal ions onto ABCP was studied using the pseudo-first order
175 (PFO) [27] (eq. 1), the pseudo-second order (PSO)[28] (eq. 2) and the Vermeulen (Ver) [29] and
176 refs. therein (eq. 3) kinetic equations:

$$\frac{dq}{dt} = k_1(q_e - q_t) \quad (1)$$

$$\frac{dq}{dt} = k_2(q_e - q_t)^2 \quad (2)$$

$$\frac{dq}{dt} = k_v\frac{(q_e^2 - q_t^2)}{q_t} \quad (3)$$

177 whose integrated form for the boundary conditions $t = 0$, $q = 0$ and $t = t$, $q = q_t$ are reported in eqs 4
178 – 6:

$$q_t = q_e(1 - e^{-k_1 t}) \quad (4)$$

$$q_t = \frac{q_e^2 k_2 t}{1 + q_e k_2 t} \quad (5)$$

$$q_t = q_e(1 - e^{-2k_v t})^{0.5} \quad (6)$$

179 where k_1, k_2 and k_v are the rate constants of adsorption, q_e is the sorption capacity at equilibrium and
180 q_t is the amount of metal adsorbed at time t.

181 The equilibrium adsorption data were fitted with different isotherm equations. In particular, the
182 Freundlich and Langmuir models [30,31] have been used in the forms reported in eqs 7-8:

$$q_e = K_F C_e^{1/n} \quad (7)$$

$$q_e = \frac{q_m K_L C_e}{1 + K_L C_e} \quad (8)$$

183 where: q_m is the maximum adsorption capacity of the material, expressed in mg g^{-1}; K_F and K_L are
184 the constants of Freundlich and Langumir models, respectively, from which information about the
185 binding capacity or affinity of the adsorbent toward the metal ion can be obtained; C_e (mg L^{-1}) is the
186 metal concentration in solution at equilibrium; n is an empirical parameter, which gives information
187 on the strength of the adsorption. Langmuir model describes the adsorption on equivalent sites of
188 the adsorbent material which can be saturated obtaining a monolayer, Freundlich model takes in to
189 account the heterogeneity of the binding sites.

190 The metal ion adsorption at different contact times t (q_t, mg g^{-1}) in the kinetic study, or at different
191 M^{2+} / ABCP ratio in the equilibrium study (q_e, mg g^{-1}) was calculated by the eq. 9:

$$q_t or\ q_e = \frac{V(C_0 - C_t)}{m} \quad (9)$$

192 where V (L) is the volume of the metal ion solution and m is the mass of ABCP (g); C_0 and C_t are

193 the metal ion concentrations in solution (mg L^{-1}) at $t = 0$ and $t = t$, respectively. At the equilibrium
194 condition, eq. 9 was applied by replacing C_t with C_e to calculate q_e.
195 The conditional Langmuir constant values (in $NaNO_3$ 0.1 mol L^{-1}; C_{Pb}^{2+} in mol L^{-1}) [32] at
196 different temperatures were used to calculate the thermodynamic parameters ΔG (kJ mol^{-1}), ΔH (kJ
197 mol^{-1}) and ΔS (kJ mol^{-1} K^{-1}) by using Gibbs and van't Hoff equations (eqs 10 and 11). The
198 following assumptions were done: i) the adsorption is reversible, ii) the stoichiometry of adsorption
199 doesn't change; iii) equilibrium condition is established during adsorption experiments [33,34].

$$\Delta G = -RT \ln K_L \quad (10)$$

$$\ln K_L = -\frac{\Delta H}{RT} + \frac{\Delta S}{R} \quad (11)$$

200 where R is the universal gas constant 0.008314 kJ mol^{-1} K^{-1} and T is the temperature in K.
201

202 3. Results and Discussions

203 *3.1 Pyrolysis experiments*

204 The pyrolysis of *Posidonia oceanica* was done at 673.15 K, 773.15 K and 873.15 K in order to
205 study the behaviour of the feedstock, at the three operative temperatures, in terms of yields of the
206 main pyrolysis product (bio-oil) and of secondary products (BCP and gas). The product yields are
207 reported in Table 1 together with standard deviations. The conversion of *Posidonia oceanica* in
208 volatiles (calculated as the sum of both bio-oil and gas yields) increases with the temperature
209 increase, while the BCP yield has an opposite trend. The highest BCP yield was obtained at 673.15
210 K (33.2 %) with a conversion in total volatiles of 66.8 wt%. An increasing of 12.6 % of conversion
211 was obtained passing from 673.15 to 873.15 K.
212 The higher percentage of gas at 873.15 K (35.7 wt%) can be attributed to secondary decomposition
213 reactions that promote CO and CO_2 release.
214 These results indicate that the increase of the operative temperature accelerates the *Posidonia*
215 *oceanica* conversion rate to condensable compounds (bio-oil) and gaseous (*i.e.* CO, CO_2, CH_4 etc...)

species. Considering the highest BCP yield obtained at 673.15 K (33.2 wt%), the BCP produced at this pyrolysis temperature was that subject to activation and adsorption/ desorption experiments.

Table 1. *Posidonia oceanica* conversion and distribution of pyrolysis products

T (K)	Conversion wt % (Total volatiles)	BCP yield %	Bio-oil yield %	Gas yield %
673.15	66.8	33.2 ± 0.1 [a]	45.5 ± 0.1 [a]	21.3 ± 0.1 [a]
773.15	75.2	24.8 ± 0.1	48.4 ± 0.1	26.8 ± 0.1
873.15	79.4	20.6 ± 0.1	43.7 ± 0.1	35.7 ± 0.1

[a] ± std. dev.

3.2 Activation and characterization of BCP

As elsewhere reported, the biochar produced from *Posidonia oceanica* contains high amounts of Ca and Mg and the pH of a BCP-water mixture is higher than 10 [7,8]. This makes it impossible the use of BCP as adsorbent material of a generic toxic metal ion whose hydrolysis usually starts at lower pH values with the formation of low soluble hydrolytic species. For this reason, the BCP chemical activation with sulfuric acid had different objectives: i) reduce the inorganic content; ii) increase the acidic functional groups of material and iii) improve its morphological properties (superficial area, pore volume, etc.).

Elemental analysis and nitrogen adsorption-desorption experiments were carried out onto the BCP (produced at 673.15 K) and the ABCP. The results are reported in Table 2 together with the elemental analysis of *Posidonia oceanica*. Both pyrolysis and chemical activation increase the carbon fraction (from 46.14 wt% to 63.66 wt%) as better highlighted by O/C ratio used to monitor the carbonization process. This behaviour can be attributable to the volatilization of oxygenated compounds that would lead to an aromaticity development mainly in the BCP structure [5,7,35,36].

The isotherm of nitrogen adsorption at 77.15 K for BCP and ABCP and the pore size distribution of both materials are shown in Figures 1 and 2, respectively.

The chemical activation of BCP above described led to a changing of superficial area, pore volume and average pore width. In particular, the superficial area and pore volume increase from 4.664 to 20.936 m^2/g and from 0.015 to 0.018 cm^3/g, respectively. On the other side, the average pore width decreased from 12.905 nm to 3.324 nm. Basically, these values reveal that both BCP and ABCP have essentially a mesopores structure; however, the ABCP sample shows a moderate shifted towards pores of smaller dimension.

Table 2. Results of elemental analysis and nitrogen adsorption-desorption measurements

	Elemental analysis [a]					
	C	**H**	**N**	**S**	**O**	**O/C**
Posidonia oceanica [b]	46.14	6.82	1.28	0.33	29.73	0.64
BCP	49.54	2.41	1.52	0.08	28.00	0.56
ABCP	63.66	3.23	2.03	0.21	12.43	0.19
	N_2 Adsorption – desorption measurements [b]					
	BCP		ABCP			
BET $m^2\ g^{-1}$	4.664		20.936			
t-Plot Micropore Area $m^2\ g^{-1}$	2.378		5.726			
Desorption average pore width (4V/A) nm	12.905		3.324			
Pore Volume $cm^3\ g^{-1}$	0.0150		0.0174			

[a] dry basis, ± 0.02. [b] ± 2 %

The low N_2 adsorbed volume (53.60 cm^3/g) observed for ABCP sample at partial pressure (P/P^0) equal to unity (see Figure 1) suggests that the activation method was not able to induce the creation of a microporous structure.

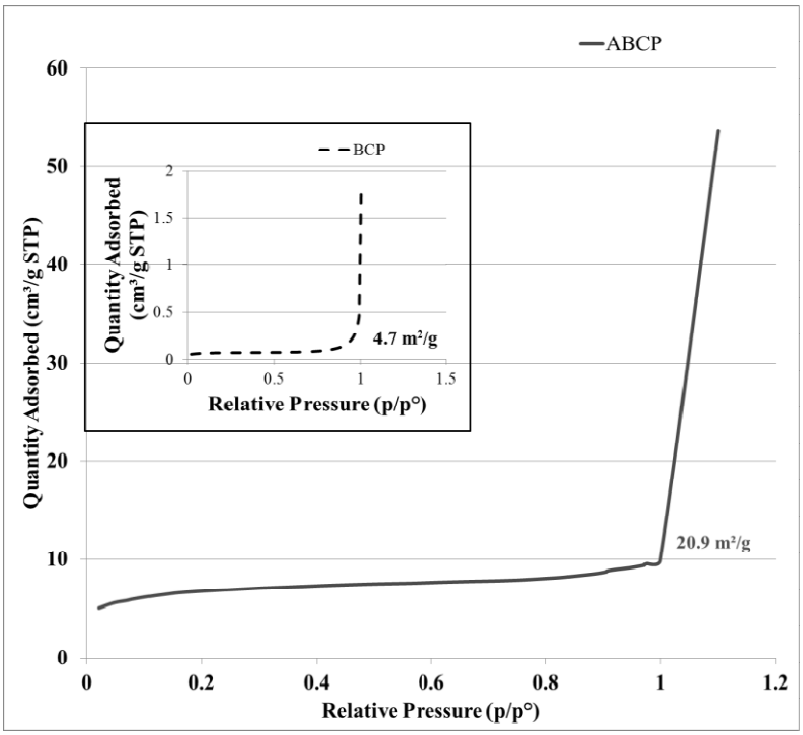

Figure 1. Adsorption isotherms of N_2 onto BCP and ABCP

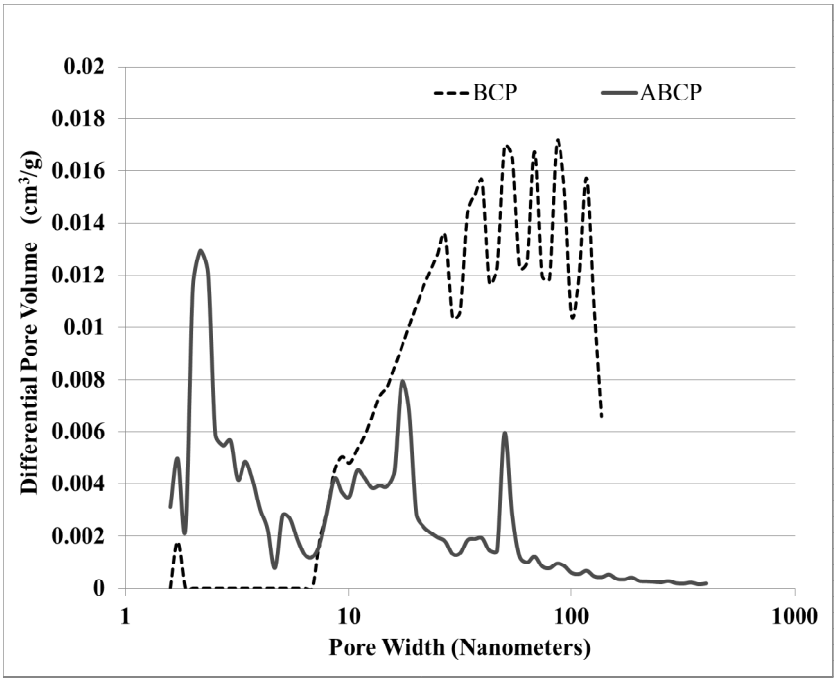

Figure 2. BJH desorption pore size distribution of BCP and ABCP

In order to monitor the textural properties and the minerals on the biochar samples, SEM analysis coupled with EDX characterization were performed. Figures 3a and 3c show the surface of the BCP

and ABCP at the same magnifications (800x). The surface of BCP appears homogeneous and without any whole and it changes after the chemical activation with an increase of porosity.

EDX spectra carried out on both BCP and ABCP samples (see Figures 3b and 3d) detected an increasing of carbon content and a decreasing of oxygen (see the At % reported in Table 3), in agreement with the elemental composition data reported in Table 2, and confirm the carbonization process promoted by activation treatment. Furthermore, due to the cleaner effect of sulfuric acid treatment, the chemical activation reduces the Ca and Mg concentrations in BCP.

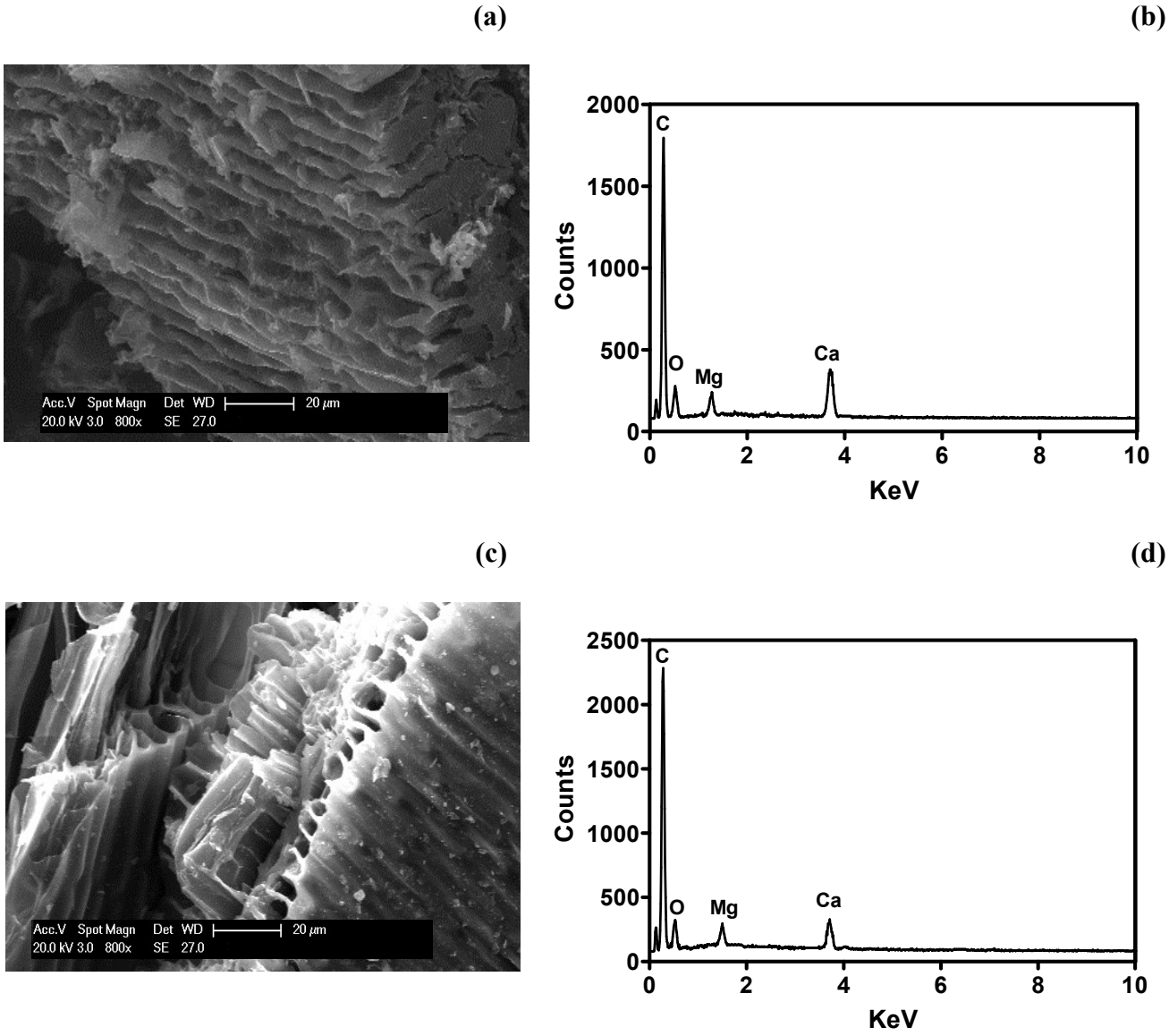

268 **Figure 3.** SEM micrographs at 800x magnification and EDX spectra of BCP (3a, 3b) and ABCP
269 (3c, 3d)

270

271 **Table 3.** EDX microanalysis of BCP and ABCP samples

Elements	BCP	ABCP
	At %	At%
C	83.43 [a]	85.52 [a]
O	12.76	9.94
Mg	1.30	0.81
Ca	3.21	2.51

272 [a] The percentages are the average of three EDX analysis with a mean error of 5%.

The pH_{pzc} of ABCP has been measured at I = 0.1 mol L^{-1}, in $NaNO_3$ and NaCl ionic media. Small differences were found at the two experimental conditions with pH_{pzc} = 6.0 and 6.1 in $NaNO_3$ and NaCl media, respectively (see Figure 1S of Supplementary Material). It means that, in the two ionic media at pH lower than ~ 6, the ABCP surface has a net positive charge, which becomes negative at pH higher than pH_{pzc}.

3.3 Modeling of kinetic of toxic metal ions uptake by ABCP

The kinetics of Pb^{2+}, Cd^{2+} and Cu^{2+} adsorption onto ABCP were studied at I = 0.1 mol L^{-1}. ($NaNO_3$), at initial pH = 5. PFO, PSO and Ver kinetic models were used to fit the experimental data. The kinetic parameters values calculated with the three equations are reported in Table 4.

From a mere statistical point of view, the Vermeulen model gave the best fit for each investigated ABCP /cation system, with the higher R^2 and the lowest std. dev. values of the fits. This is clearly shown also in Fig 2S of Supplementary Material where are reported the experimental kinetic data together with the fit curves of the three kinetic equations. On the basis of the above considerations, comments on the results of the adsorption kinetics will be based on the kinetic parameters calculated with Ver equation.

From a practical and chemical perspective, differences were found in the adsorption capacity (q_e) and the kinetic of sorption of ABCP towards Cd^{2+}, Cu^{2+} and Pb^{2+} ions. In particular, the adsorption capacity trend of ABCP towards the three metal ions is: $Cu^{2+} > Pb^{2+} > Cd^{2+}$ (q_e = 0.08, 0.05 and 0.02 mmol g^{-1} for Cu^{2+}, Pb^{2+} and Cd^{2+} ions, respectively).

The adsorption equilibrium, at the experimental conditions used, was reached within 4 hours for Cd^{2+} and Cu^{2+} adsorption, whilst, almost 16 hours were needed in the case of Pb^{2+}.

The adsorption rate of Cd^{2+} and Pb^{2+} ions is almost the same and lower than that of Cu^{2+} ions (k_v = 0.015, 0.002 and 0.005 min^{-1} for Cu^{2+}, Pb^{2+} and Cd^{2+} ions, respectively). The pH of metal ion solution at the end of kinetic experiments was almost the same of the initial pH (5 ± 0.3).

Table 4. Parameters of PFO, PSO and Ver kinetic equations for Pb^{2+}, Cu^{2+} and Cd^{2+} adsorption on ABCP, in aqueous solution containing $NaNO_3$ 0.1 mol L^{-1} and at T = 298.15 K.

Model	q_e (mg g^{-1})	k_i [a, b]	R^2	σ [c]
		Pb^{2+}		
PFO	9.5 ± 0.22	0.013 ± 0.002	0.8595	1.2199
PSO	10.2 ± 0.2	0.002 ± 0.001	0.9247	0.8929
Ver	10.1 ± 0.1	0.002 ± 0.001	0.9568	0.6763
		Cu^{2+}		
PFO	4.90 ± 0.09	0.069 ± 0.007	0.7669	0.5690
PSO	5.02 ± 0.07	0.024 ± 0.002	0.8823	0.4042
Ver	4.98 ± 0.07	0.015 ± 0.001	0.8851	0.3995
		Cd^{2+}		
PFO	1.81 ± 0.04	0.026 ± 0.003	0.8054	0.2568
PSO	1.89 ± 0.04	0.020 ± 0.003	0.8470	0.2278
Ver	1.84 ± 0.04	0.005 ± 0.001	0.8671	0.2123

[a] min^{-1} for both k_1 and k_v, g mg^{-1} min^{-1} for k_2; [b] subscript i is 1, 2 or v according to the model; [d] standard deviation of the fit.

3.4 Modeling of equilibria of toxic metal ions uptake by ABCP: effect of temperature, ionic medium and ionic strength

The equilibrium experimental data of metal ions adsorption onto ABCP were fitted with Langmuir and Freundlich isotherm equations and the parameters of the two models, reported in Tables 5 and 6, have been analyzed in order to obtain information about adsorption mechanism, affinity of the adsorbent towards adsorbates and maximum adsorption capacity. Both isotherm models fit well the experimental data with small differences in the statistical parameters R^2 and σ of the fit of each metal – adsorbent system.

At first, adsorption isotherms for the three metal ions were carried out at the same experimental conditions ($NaNO_3$ 0.1 mol L^{-1}, at pH = 5 and T = 298.15 K). The maximum adsorption capacity

trend of ABCP towards the metal ions was $Cu^{2+} > Pb^{2+} > Cd^{2+}$ (q_m = 0.112, 0.094 and 0.066 mmol g^{-1} for Cu^{2+}, Pb^{2+} and Cd^{2+} ions, respectively), whilst, the adsorbent material showed the highest affinity towards Pb^{2+} ion (K_L = 373, 15.2 and 5.6 L $mmol^{-1}$ for Pb^{2+}, Cu^{2+} and Cd^{2+}, respectively). Considering the highest affinity of ABCP towards Pb^{2+} ions and the dangerousness of this metal ion towards humans, animals and plants, the Pb^{2+} adsorption study was extended carrying out more isotherm experiments in NaCl medium, at different ionic strengths and temperatures (see Table 6).

Table 5. Parameters of Freundlich and Langmuir isotherms for the Pb^{2+} Cd^{2+} and Cu^{2+} adsorption onto ABCP from aqueous solution at pH = 5 containing $NaNO_3$ at I = 0.1 mol L^{-1} and at different temperature.

	Langmuir model				**Freundlich Model**			
T [a]	q_m [b]	K_L [c]	R^2	σ [d]	K_F [e]	***n***	R^2	σ [d]
				Pb^{2+} adsorption				
283.15	16.1 ± 0.7	1.5 ± 0.7	0.9058	1.64	10.3 ± 0.7	8 ± 1	0.9377	1.33
298.15	19.5 ± 0.2	1.8 ± 0.1	0.9994	0.49	12.0 ± 0.7	7 ± 1	0.9412	1.57
313.15	27.2 ± 0.7	2.1 ± 0.3	0.9802	1.42	16 ± 1	7 ± 1	0.9370	2.53
333.15	29.8 ± 0.6	2.4 ± 0.3	0.9850	1.27	18 ± 1	8 ± 1	0.9177	2.97
				Cu^{2+} adsorption				
298.15	7.1± 0.3	0.24 ± 0.4	0.9751	0.30	2.3± 0.2	3.2 ± 0.4	0.9592	0.38
				Cd^{2+} adsorption				
298.15	7.5 ± 0.7	0.05 ± 0.01	0.9594	0.29	0.8 ± 0.1	1.9± 0.1	0.9714	0.24

[a] in K; [b] mg g^{-1}; [c] Langmuir constant in L·mg^{-1}; [d] standard deviation of the whole fit; [e] Freundlich constant in $L^{1/n}$ g^{-1} $mg^{1-1/n}$.

In the temperature range 283.15 – 333.15 K, the adsorption ability, as well as the affinity of ABCP towards Pb^{2+} ion increase with the increasing of temperature (q_m = 16.1 and 29.8 mg g^{-1} and K_L =

1.5 and 2.4 L mg^{-1} at T = 283.15 and 333.15 K, respectively). The adsorption of Pb^{2+} onto ABCP at the four temperatures investigated together with the fit curves of Langmuir and Freundlich isotherm models are reported in Figure 3S of Supplementary Material.

The adsorption capacity of ABCP towards Pb^{2+} increases in NaCl medium (q_m = 19.5 and 38 mg g^{-1} at I = 0.1 mol L^{-1} in $NaNO_3$ and NaCl, respectively) and the amount of metal ion adsorbed increases with the increasing of NaCl concentration (q_m = 38 and 282 mg g^{-1} in NaCl, at I = 0.1 and 1.0 mol L^{-1}, respectively). This trend has been attributed to the effect of chloride concentration in solution which completely changes the Pb^{2+} speciation. The dependence of q_m on the chloride concentration is reported in Figure 5 together with the curve fit obtained with the proposed empirical equation 12.

$$q_m = q_{m0} + p\ C_{Cl}^{-1} \qquad (12)$$

where q_{m0} is the maximum amount of Pb^{2+} adsorbed by ABCP at C_{Cl}^- = 0 mol L^{-1} and p is an empirical parameter for the dependence of q_m on C_{Cl}^-. The q_{m0} and p values are equal to 13 ± 4 and 246 ± 4, respectively, with a standard deviation on the fit σ = 5.7. Considering a small effect of nitrate on the Pb^{2+} adsorption onto ABCP and the errors on the equation parameters, the q_{m0} value is in good agreement with the q_m value of 19.5 mg g^{-1} calculated in $NaNO_3$ 0.1 mol L^{-1} and T = 298.15 K.

The proportional increase of the amount of Pb^{2+} adsorbed by ABCP with the increasing of chloride concentration in solution can be explained in terms of different metal ion speciation in the solutions. In fact, considering that the pH_{pzc} of ABCP is ~ 6, at pH = 5 its surface has positive net charge and it is able to bind also Pb^{2+} species of opposite charge [$PbCl_3^-$, $Pb(OH)_3^-$]. The distribution diagrams of hydroxo and chloride species of Pb^{2+} vs. pH at the different ionic strengths have been drawn by using the formation constants reported in ref. [37]. In Figure 4S of Supplementary Material are reported the sum of positively (Pb^{2+}, $Pb(OH)^+$, $PbCl^+$), neutral [$Pb(OH)_2$, $PbCl_2$, PbClOH] and negatively [$PbCl_3^-$, $Pb(OH)_3^-$] charged Pb^{2+} species as function of C_{Cl}^- in solution at pH = 5 derived

from the distribution diagrams. As can be seen, the percent of negatively charged species goes from 0.58 to 24.14 % when the ionic strength passes from 0.1 to 1 mol L^{-1}, in perfect agreement with the increasing trend of q_m with C_{Cl^-}.

The K_L values decrease with the increasing of ionic strength of solution (K_L = 0.13 and 0.04 L mg^{-1} at I = 0.1 and 1.0 mol L^{-1}, respectively).

The same trend of q_m and K_L values with NaCl concentration was found for the Pb^{2+} adsorption onto a commercial active carbon Filtrasorb 400 [23]. As hypothesized in that work, the decrease of K_L with ionic strength can be attributable to a charge screening effect that reduces the affinity of ABCP towards Pb^{2+} ion.

Table 6. Parameters of Freundlich and Langmuir isotherms for the Pb^{2+} adsorption on biochar from aqueous solution at pH = 5 containing NaCl at different ionic strength and at T = 298.15 K.

	Langmuir model				**Freundlich Model**			
I^a	$q_m{}^b$	$k_L{}^c$	R^2	σ^d	$k_F{}^e$	n	R^2	σ^d
0.10	38 ± 3	0.13 ± 0.04	0.9496	2.58	7 ± 1	2.4 ± 0.3	0.9617	2.25
0.25	80 ± 2	0.08 ± 0.01	0.9982	0.82	12 ± 1	2.2 ± 0.1	0.9917	1.74
0.50	133 ± 11	0.08 ± 0.01	0.9893	2.69	15 ± 2	1.7 ± 0.1	0.9822	3.46
0.75	180 ± 19	0.05 ± 0.01	0.9905	2.75	13 ± 2	1.5 ± 0.1	0.9809	3.89
1.00	282 ± 32	0.04 ± 0.01	0.9960	1.80	13.8 ± 0.9	1.25 ± 0.05	0.9931	2.35

[a] in mol·L^{-1}; [b] mg g^{-1}; [c] Langmuir constant in L·mg^{-1}; [d] standard deviation of the whole fit; [e] Freundlich constant in $L^{1/n}$ g^{-1} $mg^{1-1/n}$.

The pH of each metal ion solutions, initially 5, was measured after batch isotherm experiments. The variation of pH was not significant considering that the maximum changing was of 0.3 units.

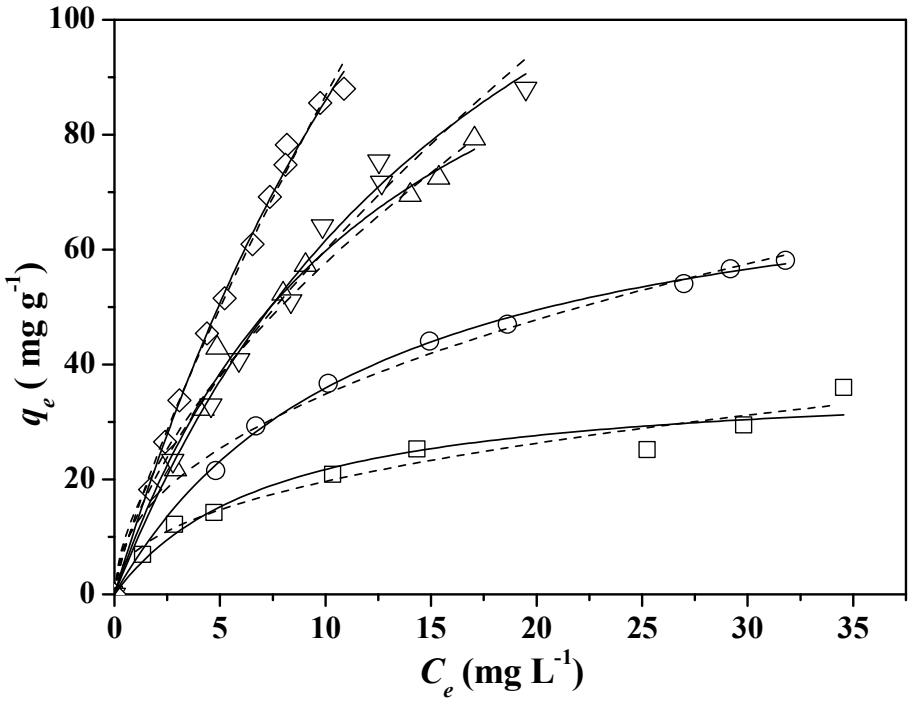

372

373 **Figure 4.** Adsorption isotherms of Pb^{2+} onto ABCP from aqueous solutions at pH = 5 containing

374 NaCl 0.10 (□), 0.25 (○), 0.50 (△), 0.75 (▽) and 1.00 (◇) mol L^{-1} and at T = 298.15 K.

375 Experimental data fitted with Freundlich (dotted lines) and Langmuir (continuous lines) models.

376

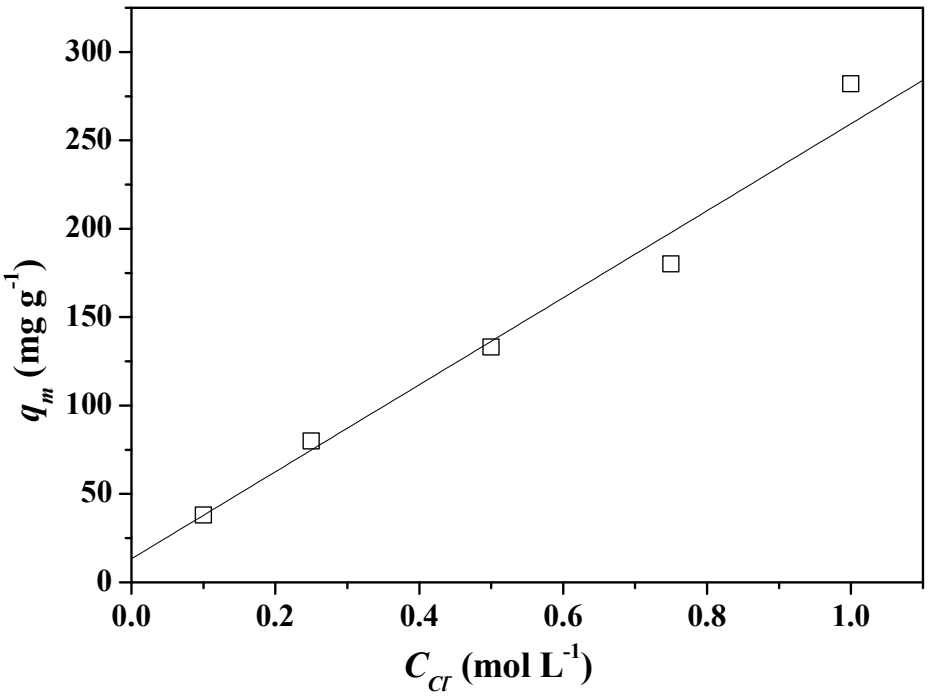

Figure 5. Dependence of q_m on C_{Cl^-} for the adsorption of Pb^{2+} onto ABCP at T = 298.15 K. The q_m value at C_{Cl^-} = 0 (q_{m0}) was calculated by using experimental q_m values and applying eq. 12.

3.5 Thermodynamic parameters of Pb^{2+} adsorption onto ABCP

Conditional K_L values calculated in $NaNO_3$ medium at I = 0.1 mol L^{-1} at different temperatures in the range 283.15 – 333.15 K were used to calculate thermodynamic parameters, ΔG, ΔH and ΔS by using Gibbs and van't Hoff equations. The values of thermodynamic parameters are reported in Table 7 together with the ΔG values calculated in NaCl medium at different ionic strengths.

The Pb^{2+} adsorption onto ABCP is a spontaneous process, with negative ΔG values that decrease from -29.8 to -36.3 kJ mol^{-1} with the increasing of temperature from 283.15 to 333.15 K.

The adsorption process is endothermic (ΔH = 7.4 kJ mol^{-1}) and characterized by a small and positive ΔS (0.13 kJ mol^{-1} K^{-1}). It means an increasing degree of freedom of Pb^{2+} in solution and a dissociative mechanism of adsorption [33]. Moreover, an increasing of randomness in the solid-solution interface is supposed [33,38] . Although a positive enthalpy change is usually associated to chemisorption [33], as confirmed by IUPAC [39], it is not possible to do a sharp distinction

between chemical and physical adsorption. Both adsorption mechanisms can occur simultaneously and, as consequence, the strength of interaction between adsorbent and adsorbate will be different. It could be the reason of the lower amount of Pb^{2+} desorbed during desorption steps of the recycling experiments respect to Pb^{2+} adsorbed (see section 3.6). Moreover, the strength of interaction between ABCP and Pb^{2+} depends on the speciation of metal ion which in turn depends on the experimental conditions of solution (ionic medium, ionic strength, pH).

Table 7. Thermodynamic parameters ΔG, ΔH and ΔS for the Pb^{2+} adsorption onto ABCP from aqueous solution at pH = 5, in different ionic media, ionic strengths and temperatures

***T* (K)**	**Medium**	***I* (mol L^{-1})**	**$-\Delta G$[a]**	**ΔH [a]**	**ΔS [b]**
283.15			29.8 ± 0.5	7.4 ± 0.4	0.13 ± 0.01
298.15			31.8 ± 0.5		
313.15	$NaNO_3$	0.10	33.8 ± 0.5		
333.15			36.3 ± 0.4		
		0.10	25.3 ± 0.8		
		0.25	24.1 ± 0.3		
298.15	NaCl	0.50	24.1 ± 0.3		
		0.75	22.9 ± 0.5		
		1.00	22.4 ± 0.6		

[a] kJ mol^{-1}; [b] kJ mol^{-1} K^{-1}

3.6 Recycling and reuse of ABCP

Recycling tests were carried out in column as reported in section 2.3. Four adsorption-desorption steps were done and the results are reported in Figure 6.

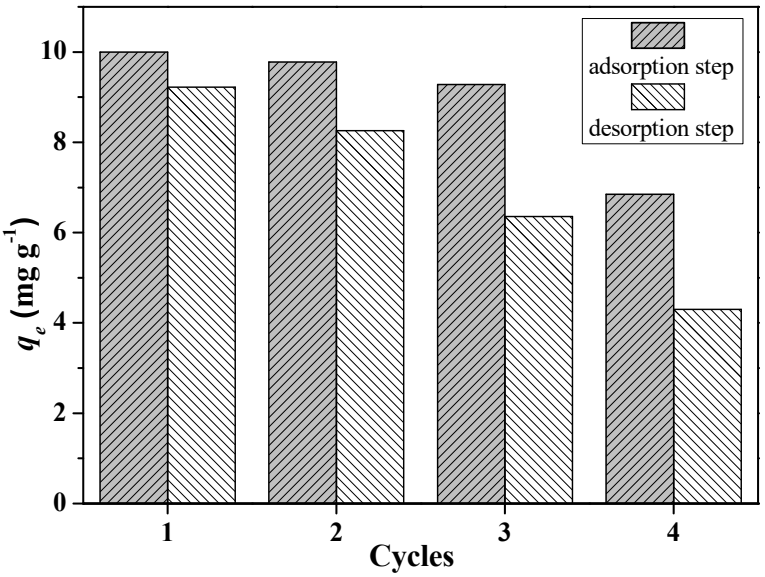

Figure 6. q_e values of adsorption - desorption steps. Experimental details: amount of ABCP in column = 0.5 g; Pb^{2+} solution: C_{Pb}^{2+} = 60 mg L^{-1}, pH = 5, in NaCl 0.1 mol L^{-1}; extractant solution: C_{HNO_3} = 0.1 mol L^{-1}.

As can be seen, in the first three cycles, the amount of Pb^{2+} adsorbed is almost 10 mg g^{-1}. The adsorbent shows a good reuse capacity even if the amount of Pb^{2+} desorbed gradually decreases with the increase of the cycle number. In particular, the Pb^{2+} desorbed at the fourth cycle is almost half of that of the first desorption step. It can be attributable to the different strength of interaction between ABCP and Pb^{2+} ions. In fact, it must be considered that, at the experimental conditions of aqueous solution used in the recycling test, the metal ion is present as positively, negatively and neutral species (see section 3.4 and Figure 4S of Supplementary Material).

3.7 Comparison with literature data

The adsorption ability of a biochar towards metal ions, as well as that of all adsorbent materials, depends on many variables related to the biochar (type of biomass used, temperature of pyrolysis, activation procedure, etc) and to the aqueous solution containing the metal ions (pH, ionic medium,

ionic strength, temperature) and the results obtained in this work confirm how the temperature, the ionic medium and the ionic strength can dramatically change the adsorption ability and the affinity of ABCP towards Pb^{2+} ions. For this reasons, comparison with literature data is very difficult because of different experimental conditions adopted by authors or because the lack of information about the characteristics of metal ion solutions used in the experiments. Moreover, to our knowledge, no data regarding the adsorption properties of biochar produced from pyrolysis of *Posidonia oceanica* towards metal ions are reported in literature. However, a rough comparison with biochars produced by algal biomasses can be done. Jeyakumar *et al.* used an activated biochar obtained from pyrolysis at 1073.15 K of *Ulva fasciata* previously treated with $CaCl_2$, Na_2CO_3 or Na_2SO_4 solutions. They found q_m values in the range 22.935 – 24.154 mg g^{-1} at pH = 4, without ionic medium and at T = 301.15 K [40], very similar to 19.5 mg g^{-1} found in this work at pH = 5, in the lower interacting medium $NaNO_3$ and at T = 313.15 K. Ibrahim *et al.* studied the adsorption of Cu^{2+}, Cd^{2+} and Pb^{2+} onto biochar from *Ulva fasciata* activated with KOH at 1073.15 K [41]. They found q_m values of 84.7, 84.6 and 83.3 mg g^{-1} for Cu^{2+}, Cd^{2+} and Pb^{2+} ions, respectively, at pH = 5. The different adsorption ability of this biochar towards the three metal ions respect to those found in this work, can be justified by considering the differences in the experimental conditions evidenced in the first part of this section. The same considerations can be done for the q_m value of 146.85 mg g^{-1} found by Li *et al.* for the Pb^{2+} adsorption onto activated biochar from *Enteromorpha prolifera* at pH = 5 and T = 298.15 K [42].

3.8 Conclusions

Recently, dead *Posidonia oceanica* residues collected from the southwestern coast of Sicily region (Italy) were used as biomass in pyrolysis processes for bio-oil production [7,8]. The large amount of biochar produced during the pyrolysis is usually considered a byproduct of the process that, consequently, has to be disposed. With the aim of transforming the biochar from byproduct to high value-added material, in this work it was tested as adsorbent material towards toxic metal ions.

To this end, firstly the biochar was chemically activated and characterized. Then the ABCP was used to remove Cu^{2+}, Cd^{2+} and Pb^{2+} ions from aqueous solutions fixing the pH at 5. The kinetic and thermodynamic of metal ion adsorption were studied evaluating the effect of important variables of the metal – biochar systems investigated (ionic medium, ionic strength, temperature).

The results obtained can be summarized as follows:

1. the chemical activation improved the adsorption ability of biochar towards metal ions;
2. The ABCP is a good adsorbent material of Pb^{2+} ($0.077 \leq q_m$ (mmol g^{-1}) ≤ 1.361), Cd^{2+} (q_m = 0.066 mmol g^{-1}) and Cu^{2+} (q_m = 0.112 mmol g^{-1}) ions in the experimental conditions considered;
3. among kinetic models, the Vermeulen equation gave the best fit for each investigated ABCP /cation system; the adsorption equilibrium was reached within 4 hours for Cd^{2+} and Cu^{2+} adsorption, whilst, almost 16 hours were needed in the case of Pb^{2+};
4. on the basis of K_L and q_m values of Langmuir model, ABCP has a higher affinity towards Pb^{2+} ions with the following maximum adsorption capacity trend: $Cu^{2+} > Pb^{2+} > Cd^{2+}$;
5. the amount of Pb^{2+} adsorbed by ABCP (q_m) is higher in NaCl than in $NaNO_3$ and it increases with the increasing of chloride concentration in solution; this behavior was explained in terms of metal ion speciation in solution and an empirical equation was proposed to describe it;
6. the Pb^{2+} adsorption onto ABCP is a spontaneous (negative ΔG values) and endothermic process (ΔH = 7.4 kJ mol^{-1}). Moreover it is characterized by a small and positive ΔS (0.13 kJ mol^{-1} K^{-1}). An adsorption mechanism based on simultaneous chemical and physical interactions has been supposed;
7. ABCP can be reused for at least four adsorption/desorption cycles by using hydrochloric acid solution 0.1 mol L^{-1} to desorb the metal ion as confirmed by the column recycling tests;
8. the sorption ability of ABCP, considering the different experimental conditions of pyrolysis and activation of biochar and of the metal ions solutions, is of the same order of magnitude of other activated biochars from algal biomasses reported in literature.

Acknowledgements

We thank the Italian Ministero dell'Istruzione, dell'Università e della Ricerca (MIUR, PRIN project n. 2015MP34H3_003 and 2015MP34H3_004) for financial support.

References

[1] A. Demirbaş, Oily Products from Mosses and Algae via Pyrolysis, Energy Sources Part Recovery Util. Environ. Eff. 28 (2006) 933–940. doi:10.1080/009083190910389.

[2] P. Pan, C. Hu, W. Yang, Y. Li, L. Dong, L. Zhu, D. Tong, R. Qing, Y. Fan, The direct pyrolysis and catalytic pyrolysis of Nannochloropsis sp. residue for renewable bio-oils, Bioresour. Technol. 101 (2010) 4593–4599. doi:10.1016/j.biortech.2010.01.070.

[3] D. Li, L. Chen, X. Yi, X. Zhang, N. Ye, Pyrolytic characteristics and kinetics of two brown algae and sodium alginate, Bioresour. Technol. 101 (2010) 7131–7136. doi:10.1016/j.biortech.2010.03.145.

[4] K. Chaiwong, T. Kiatsiriroat, N. Vorayos, C. Thararax, Study of bio-oil and bio-char production from algae by slow pyrolysis, Biomass Bioenergy. 56 (2013) 600–606. doi:10.1016/j.biombioe.2013.05.035.

[5] S. Grierson, V. Strezov, G. Ellem, R. Mcgregor, J. Herbertson, Thermal characterisation of microalgae under slow pyrolysis conditions, J. Anal. Appl. Pyrolysis. 85 (2009) 118–123. doi:10.1016/j.jaap.2008.10.003.

[6] S. Grierson, V. Strezov, P. Shah, Properties of oil and char derived from slow pyrolysis of Tetraselmis chui, Bioresour. Technol. 102 (2011) 8232–8240. doi:10.1016/j.biortech.2011.06.010.

[7] S. Maisano, F. Urbani, N. Mondello, V. Chiodo, Catalytic pyrolysis of Mediterranean sea plant for bio-oil production, Int. J. Hydrog. Energy. 42 (2017) 28082–28092. doi:10.1016/j.ijhydene.2017.07.124.

[8] V. Chiodo, G. Zafarana, S. Maisano, S. Freni, F. Urbani, Pyrolysis of different biomass: Direct comparison among Posidonia Oceanica, Lacustrine Alga and White-Pine, Fuel. 164 (2016) 220–227. doi:10.1016/j.fuel.2015.09.093.

[9] T.A. Le, H.V. Ly, J. Kim, Catalytic Pyrolysis of Alga Saccharina japonica Using Co/γ-Al2O3 and Ni/γ-Al2O3 Catalyst, Energy Sources Part Recovery Util. Environ. Eff. 36 (2014) 2392–2400. doi:10.1080/15567036.2013.839763.

[10] K. Wang, R.C. Brown, Catalytic pyrolysis of microalgae for production of aromatics and ammonia, Green Chem. 15 (2013) 675–681. doi:10.1039/C3GC00031A.

[11] K. Qian, A. Kumar, H. Zhang, D. Bellmer, R. Huhnke, Recent advances in utilization of biochar, Renew. Sustain. Energy Rev. 42 (2015) 1055–1064. doi:10.1016/j.rser.2014.10.074.

[12] M.E. Doumer, A. Rigol, M. Vidal, A.S. Mangrich, Removal of Cd, Cu, Pb, and Zn from aqueous solutions by biochars, Environ. Sci. Pollut. Res. 23 (2016) 2684–2692. doi:10.1007/s11356-015-5486-3.

[13] X. Tan, Y. Liu, G. Zeng, X. Wang, X. Hu, Y. Gu, Z. Yang, Application of biochar for the removal of pollutants from aqueous solutions, Chemosphere. 125 (2015) 70–85. doi:10.1016/j.chemosphere.2014.12.058.

[14] X. Cao, L. Ma, Y. Liang, B. Gao, W. Harris, Simultaneous immobilization of lead and atrazine in contaminated soils using dairy-manure biochar, Environ. Sci. Technol. 45 (2011) 4884–4889. doi:10.1021/es103752u.

[15] M.H. Duku, S. Gu, E.B. Hagan, Biochar production potential in Ghana—A review, Renew. Sustain. Energy Rev. 15 (2011) 3539–3551. doi:10.1016/j.rser.2011.05.010.

[16] M. Vithanage, A.U. Rajapaksha, M. Zhang, S. Thiele-Bruhn, S.S. Lee, Y.S. Ok, Acid-activated biochar increased sulfamethazine retention in soils, Environ. Sci. Pollut. Res. 22 (2015) 2175–2186. doi:10.1007/s11356-014-3434-2.

[17] Z. Xiong, Z. ShiHong, Y. HaiPing, F. Ye, C. YingQuan, W. XianHua, C. HanPing, Nitrogen enriched biochar modified by high temperature CO2-ammonia treatment: characterization and adsorption of CO2., Chem. Eng. J. 257 (2014) 20–27.

[18] S. Cataldo, A. Gianguzza, D. Milea, N. Muratore, A. Pettignano, S. Sammartano, A critical approach to the toxic metal ion removal by hazelnut and almond shells, Environ. Sci. Pollut. Res. 25 (2018) 4238–4253. doi:10.1007/s11356-017-0779-3.

[19] S. Cataldo, N. Muratore, S. Orecchio, A. Pettignano, Enhancement of adsorption ability of calcium alginate gel beads towards Pd(II) ion. A kinetic and equilibrium study on hybrid Laponite and Montmorillonite-alginate gel beads, Appl. Clay Sci. 118 (2015) 162–170. doi:10.1016/j.clay.2015.09.014.

[20] S. Cataldo, G. Lazzara, M. Massaro, N. Muratore, A. Pettignano, S. Riela, Functionalized halloysite nanotubes for enhanced removal of lead(II) ions from aqueous solutions, Appl. Clay Sci. 156 (2018) 87–95. doi:10.1016/j.clay.2018.01.028.

[21] S. Cataldo, A. Gianguzza, A. Pettignano, I. Villaescusa, Mercury(II) removal from aqueous solution by sorption onto alginate, pectate and polygalacturonate calcium gel beads. A kinetic

and speciation based equilibrium study, React. Funct. Polym. 73 (2013) 207–217. doi:10.1016/j.reactfunctpolym.2012.10.005.

[22] S. Cataldo, A. Gianguzza, A. Pettignano, Sorption of Pd(II) ion by calcium alginate gel beads at different chloride concentrations and pH. A kinetic and equilibrium study Sorption of Pd(II) ion by calcium alginate gel beads, Arab. J. Chem. 9 (2016) 656–667. doi:10.1016/j.arabjc.2014.10.031.

[23] S. Cataldo, A. Gianguzza, D. Milea, N. Muratore, A. Pettignano, Pb(II) adsorption by a novel activated carbon – alginate composite material. A kinetic and equilibrium study, Int. J. Biol. Macromol. 92 (2016) 769–778. doi:10.1016/j.ijbiomac.2016.07.099.

[24] T.R. Crompton, Toxicants in Aqueous Ecosystems: A Guide for the Analytical and Environmental Chemist, Springer-Verlag, Berlin Heidelberg, 2007. //www.springer.com/us/book/9783540357384 (accessed July 11, 2018).

[25] M. Jaishankar, T. Tseten, N. Anbalagan, B.B. Mathew, K.N. Beeregowda, Toxicity, mechanism and health effects of some heavy metals, Interdiscip. Toxicol. 7 (2014) 60–72. doi:10.2478/intox-2014-0009.

[26] S.K. Milonjić, A.L. Ruvarac, M.V. Šušić, The heat of immersion of natural magnetite in aqueous solutions, Thermochim. Acta. 11 (1975) 261–266. doi:10.1016/0040-6031(75)85095-7.

[27] S. Lagergren, About the Theory of so Called Adsorption of Soluble Substances, K. Sven. Vetenskapsakademiens Handl. 24 (1898) 1–39.

[28] G. Blanchard, M. Maunaye, G. Martin, Removal of heavy metals from waters by means of natural zeolites, Water Res. 18 (1984) 1501–1507. doi:10.1016/0043-1354(84)90124-6.

[29] F.G. Helfferich, Principles of adsorption & adsorption processes, by D. M. Ruthven, John Wiley & Sons, 1984, xxiv + 433 pp, AIChE J. 31 (n.d.) 523–524. doi:10.1002/aic.690310335.

[30] I. Langmuir, The Adsorption of Gases on Plane Surfaces of Glass, Mica and Platinum., J. Am. Chem. Soc. 40 (1918) 1361–1403. doi:10.1021/ja02242a004.

[31] H.M.F. Freundlich, Over the adsorption in solution, J Phys Chem. 57 (1906) 385–471.

[32] Y. Liu, Is the Free Energy Change of Adsorption Correctly Calculated?, J. Chem. Eng. Data. 54 (2009) 1981–1985. doi:10.1021/je800661q.

[33] H.N. Tran, S.-J. You, H.-P. Chao, Thermodynamic parameters of cadmium adsorption onto orange peel calculated from various methods: A comparison study, J. Environ. Chem. Eng. 4 (2016) 2671–2682. doi:10.1016/j.jece.2016.05.009.

[34] G. Crini, P.-M. Badot, Application of chitosan, a natural aminopolysaccharide, for dye removal from aqueous solutions by adsorption processes using batch studies: A review of

recent literature, Prog. Polym. Sci. 33 (2008) 399–447. doi:10.1016/j.progpolymsci.2007.11.001.

[35] T. Mimmo, P. Panzacchi, M. Baratieri, C.A. Davies, G. Tonon, Effect of pyrolysis temperature on miscanthus (Miscanthus × giganteus) biochar physical, chemical and functional properties, Biomass Bioenergy. 62 (2014) 149–157. doi:10.1016/j.biombioe.2014.01.004.

[36] K.A. Spokas, Review of the stability of biochar in soils: predictability of O:C molar ratios, Carbon Manag. 1 (2010) 289–303. doi:10.4155/cmt.10.32.

[37] S. Cataldo, G. Lando, D. Milea, S. Orecchio, A. Pettignano, S. Sammartano, A novel thermodynamic approach for the complexation study of toxic metal cations by a landfill leachate, New J. Chem. 42 (2018) 7640–7648. doi:10.1039/c7nj04456a.

[38] Y. Liu, Y.-J. Liu, Biosorption isotherms, kinetics and thermodynamics, Sep. Purif. Technol. 61 (2008) 229–242. doi:10.1016/j.seppur.2007.10.002.

[39] D.H. Everett, Manual of Symbols and Terminology for Physicochemical Quantities and Units, Appendix II: Definitions, Terminology and Symbols in Colloid and Surface Chemistry, Pure Appl. Chem. 31 (1972) 586–587. doi:10.1351/pac197231040577.

[40] R.P.S. Jeyakumar, V. Chandrasekaran, Adsorption of lead(II) ions by activated carbons prepared from marine green algae: Equilibrium and kinetics studies, Int. J. Ind. Chem. 5 (2014) 2. doi:10.1186/2228-5547-5-2.

[41] W.M. Ibrahim, A.F. Hassan, Y.A. Azab, Biosorption of toxic heavy metals from aqueous solution by Ulva lactuca activated carbon, Egypt. J. Basic Appl. Sci. 3 (2016) 241–249. doi:10.1016/j.ejbas.2016.07.005.

[42] Y. Li, Q. Du, X. Wang, P. Zhang, D. Wang, Z. Wang, Y. Xia, Removal of lead from aqueous solution by activated carbon prepared from Enteromorpha prolifera by zinc chloride activation, J. Hazard. Mater. 183 (2010) 583–589. doi:10.1016/j.jhazmat.2010.07.063.